

Geodetic strain in peninsular Italy between 1875 and 2001

I. Hunstad,¹ G. Selvaggi,¹ N. D'Agostino,¹ P. England,² P. Clarke,³ and M. Pierozzi⁴

Received 14 October 2002; revised 9 December 2002; accepted 21 January 2003; published 25 February 2003.

[1] We determine geodetic strain in peninsular Italy by the GPS reoccupation of the first order triangulation network of Italy installed from 1860. The uncertainties in the original measurements (about 3 ppm), and the time span between the two observations, imply that tectonic signals larger than about 0.03 ppm/yr are resolvable. Along the Apenninic belt, where the largest earthquakes are concentrated, the geodetic deformation has a clear and consistent strain pattern between adjacent regions, well above the uncertainties, and shows a pervasive NE-SW extension. Along the Tyrrhenian and Adriatic coasts the geodetic signal is not homogeneous and is comparable with the uncertainty in the original measurements. Seismic deformation, calculated over the same time interval, agrees well with estimated extensional direction, but the magnitudes of geodetic and seismic strain differ suggesting that, in part of the Apennines, significant strain accumulation over the past 130 years may not have been released in earthquakes. *INDEX TERMS:* 1242 Geodesy and Gravity: Seismic deformations (7205); 1243 Geodesy and Gravity: Space geodetic surveys; 8109 Tectonophysics: Continental tectonics—extensional (0905). *Citation:* Hunstad, I., G. Selvaggi, N. D. Agostino, P. England, P. Clarke, and M. Pierozzi, Geodetic strain in peninsular Italy between 1875 and 2001, *Geophys. Res. Lett.*, 30(4), 1181, doi:10.1029/2002GL016447, 2003.

1. Introduction

[2] The Italian peninsula is located in the broad plate boundary zone between the Eurasian and African plates [McKenzie, 1972]. Despite the overall convergence within this zone, the present tectonic regime of Italy is dominated by NE-SW extension perpendicular the axis of the Apennines. Estimates of the extension rate evaluated from summation of seismic moment tensors of recent and historical earthquakes range from 0.3 mm/yr in the northern Apennines to 2.0 mm/a in the central and southern Apennines [Selvaggi, 1998], though earlier estimates have ranged from 3 mm/yr to as high as 10 mm/yr [Westaway, 1992], with differences between these estimate reflecting different choices of seismic catalogue and M_s - M_0 relationship. Existing geodetic measurements suggest that between 3–6 mm/yr of extension takes place across the Apennines, but with only limited information on whether the strain is localized in regions of active faulting [D'Agostino *et al.*, 2001; Anzidei *et al.*, 2001]. In this paper we evaluate active crustal deformation in the Italian peninsula over time span of 126

years. We compare original angular observations from the first-order Italian triangulation network established in 1860 with the GPS positions of surviving geodetic sites. We discuss our results in the context of the regional tectonic activity and compare geodetic strain rates with rates of seismic strain release over the same time interval.

2. The 1875 Geodetic Network and the 2001 GPS Survey

[3] The Italian first-order triangulation network has been firstly established by IGM (Istituto Geografico Militare) between 1869 and 1881, when 90% of the 203 vertices which ultimately formed the network, had been established and measured. In this paper, we shall refer to this network by the date of the average of the 19th century measures (1875), and neglect the strains that occurred during the course of the first-order measurements, because 90% of the observations were taken within 6 years (5%) of the mean date. Angles between vertices were measured with a nominal precision of about one second of arc [Surace, 1992]. The baseline length of the network is between 30 to 50 km in peninsular Italy, suitable for the detection of tectonic strain. The nominal precision is equivalent to about 3 ppm, suggesting that the expected extension of a few millimetres per year across the Apennines may be significantly above the noise level.

[4] Site selection and analysis of sites documentation has been previously described in Hunstad and England [1999]. Records of monument maintenance show that many of the original monuments have been rebuilt over their correct marks, located on bedrock about 1 metre below the surface, with a precision that yields a positional uncertainty that is small compared with the uncertainties in the original angular measurements. Field inspections revealed that 103 of the original 203 pillars were in a condition suitable for reoccupation (Figure 1).

[5] Between July 2001 and June 2002, we reoccupied 51 of these 103 vertices, using GPS double frequency receivers. Seven vertices were occupied for three or more 24-hour sessions, 37 with two 8-hour sessions and the remaining 7 vertices with single 8-hour sessions.

[6] For every observing session, data from the IGM geodetic sites were integrated with Italian ASI (Agenzia Spaziale Italiana, ftp://geodaf/mt.asi.it) permanent GPS stations, providing an average of 20 sites for each daily processing session. All GPS processing was performed using the GIPSY software from the NASA Jet Propulsion Laboratory [Zumberge *et al.*, 1997]. Precise orbits, clock corrections and transformation parameters from the free-network to the ITRF2000 reference frame have been retrieved from the JPL ftp site (sideshow.jpl.nasa.gov). Because of the time-span (from June 2001 to June 2002) required for the remeasurement of the IGM sites, the final multi-session network solution was calculated by combin-

¹Istituto Nazionale di Geofisica e Vulcanologia, Rome, Italy.

²Department of Earth Sciences, Oxford University, Oxford, UK.

³School of Civil Engineering and Geosciences, Newcastle, UK.

⁴Istituto Geografico Militare, Florence, Italy.

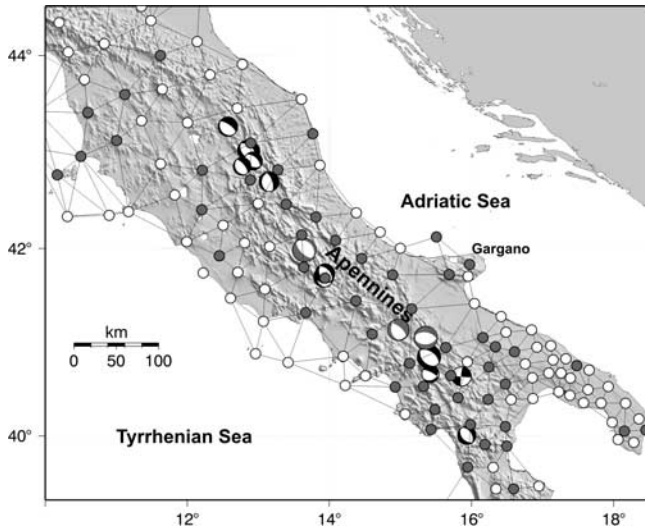


Figure 1. First order triangulation network measured between 1860 and 1890 by IGM. Dark grey circles are the sites occupied between 2001 and 2002 with GPS, and white circles are missing geodetic sites. Also shown are the original lines of sight connecting the geodetic monuments and the available fault plane solutions of the $M > 5.8$ earthquakes that occurred during the interval 1875–2002 (black focal mechanisms are CMT solutions, grey focal mechanisms are from body-wave or geodetic modelling).

ing daily solutions after a 7-parameter Helmert transformation to a reference daily solution. This reference day was chosen to minimize the residuals of the final multi-session combination. Residuals of the horizontal coordinates between the final solution and the transformed daily solutions are shown in Figures 2a and 2b.

[7] The 1875 geodetic network dataset includes only angle observations and no information on scale and orientation. We calculated coordinates for the 1875 network by assigning to two 1875 stations (LAVA and COLA, Figure 3) their 2001 coordinates and performing a network adjustment with the software Geodetic Suite [Cross, 1995]. An estimate of the quality of the original angle observation derives from the distribution of residuals between observed and calculated angles after adjustment (Figure 2c). These are normally distributed with a standard deviation of 0.6 second of arc, corresponding to 3 ppm, (i.e. about 100 mm on a 30 km long baseline).

3. Strain Analysis

[8] The methodology for evaluating tectonic strain in geodetic networks without information on scale and orientation has been established by Frank [1966]. The deformation parameters independent from any assumption of scale and orientation are the shear strains (γ_1 , γ_2) and the orientation of the greatest horizontal principal axis of the strain tensor, θ :

$$\gamma_1 = \frac{\partial u_1}{\partial x_1} - \frac{\partial u_2}{\partial x_2} \quad \gamma_2 = \frac{\partial u_1}{\partial x_2} + \frac{\partial u_2}{\partial x_1} \quad (1)$$

$$\tan 2\theta = \frac{\gamma_2}{\gamma_1} \quad (2)$$

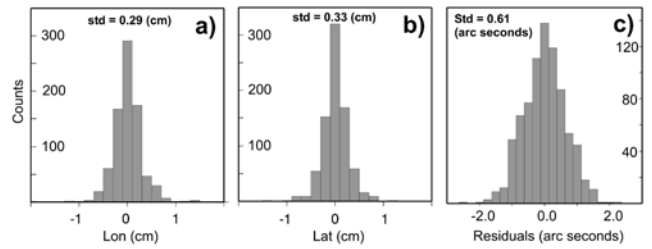


Figure 2. Residuals ((a) lon; (b) lat) of the horizontal coordinates between the final solution and the transformed GPS daily solutions. (c) Residuals between observed and calculated angles of the 1875 triangulation network.

where $\partial u_i / \partial x_j$ are the components of the displacement gradient tensor. A positive γ_1 corresponds to extension along x_1 or contraction along x_2 or a combination of both. A positive γ_2 corresponds to right-lateral shear along the x_1 direction and/or left-lateral shear along the x_2 direction. We cannot measure displacements, because of the lack of a scale or orientation in the original network, but our adjustment of the network, holding two 1875 sites fixed to their 2001 positions, allows us to calculate apparent displacements that yield shear strains and principal axes orientations identical to the full displacement field [Frank, 1966].

[9] Because of the elongate form of the Apennines, we choose our coordinate axes such that the x_1 axis is perpendicular to, and x_2 parallel to, the axis of the mountain belt (Figure 3). A second motivation for this choice of coordinate frame is that active faults predominantly show extension on NW-SE oriented planes, which is equivalent to γ_1 shear strain with negligible γ_2 shear strain. In the absence of seismological or geological evidence for significant extension or contraction parallel to the axis of the Apennines, we assume in what follows that the γ_1 strains reflect only extension or contraction in the x_1 direction; thus positive and negative values of γ_1 may be correlated to extensional and contrac-

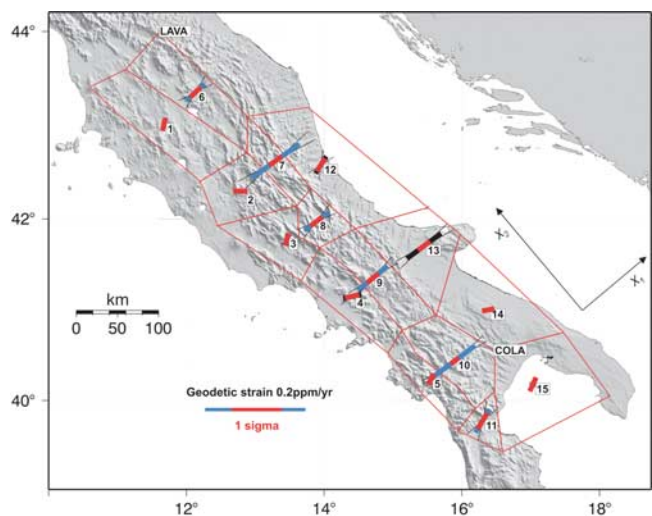


Figure 3. Positive (blue bars) and negative (black) γ_1 shear strain rates for polygonal areas discussed in the text, plotted in the direction of maximum and minimum extension respectively. The red part of the bars represents 1σ error. Thin lines define the uncertainty in the azimuth of the principal strain rate axes.

tional strain, respectively, in the NE-SW direction. Irrespective of this assumption, γ_2 shear strain represents strike-slip motion perpendicular or parallel to the Apennine belt.

[10] To minimise the possible contribution of local site instabilities and obtain more reliable strain parameters, we subdivided the study area into polygonal regions. In each polygon we estimated the four components of the horizontal displacement gradient tensor from the apparent displacements of sites on the border of and within the polygons, using a weighted least square approach. Uncertainties were propagated using the complete displacement covariance matrix.

[11] Using standard uniform slip dislocation modelling, we removed the coseismic signal at our sites for all seismic events in the interval 1875–2001 with $M > 6.0$ for which a reliable source mechanisms is available [Valensise and Pantosti, 2001]. Removing these site displacements from the observed apparent displacements yielded strain parameters that are statistically indistinguishable from those obtained using the uncorrected displacements. We therefore do not consider further the influence of coseismic deformation on our observations.

[12] In Figure 3, bars showing the magnitude of γ_1 in each polygonal region is plotted parallel to the orientation of the greatest horizontal principal axis (for positive γ_1), and of the least horizontal principal axis (for negative γ_1). The polygons have been chosen so as to subdivide three main belts: the Tyrrhenian side, the Apennine axis and the Adriatic coast. The results we present below are stable and not dependent on single site instabilities. This was tested by varying the choice of sites assigned to each polygon, in so far as is consistent with maintaining the regionalisation that is dictated by the geology. Further support for this test comes from the statistics of the polygonal strain determinations. The standard error in the

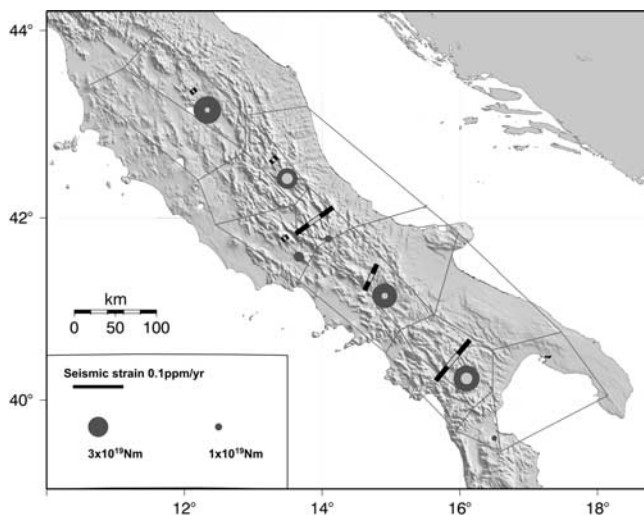


Figure 4. Orientations of principal seismic strain axes calculated from the past hundred years' major earthquakes [Selvaggi, 1998]. Light grey bars show an assumed uncertainty of 30% in the moment rate. Circles indicate the difference between the equivalent geodetic moment for each polygon (Equation 3), and the seismic moment released in earthquakes over the same time interval. Dark grey and light grey circles are the maximum and minimum discrepancy between geodetic and seismic moments, respectively.

Table 1. Shear Strains and Principal Axes (Calculated Using Equations 1 and 2) For the Polygons Regions Shown in Figure 3

Poly.	γ_1 (ppm/yr)	1σ	γ_2 ppm/yr	1σ	Az. ϵ_{\max}	1σ
1	0.0057	0.027	0.019	0.023	77	74
2	0.0037	0.029	-0.038	0.024	358	42
3	0.018	0.026	0.037	0.027	72	33
4	-0.038	0.029	0.052	0.024	13	22
5	0.024	0.025	0.023	0.022	62	35
6	0.050	0.029	0.005	0.028	43	17
7	0.116	0.032	-0.019	0.028	36	7
8	0.058	0.030	0.005	0.029	38	15
9	0.077	0.029	-0.0003	0.023	40	8
10	0.101	0.020	0.011	0.018	37	5
11	0.054	0.038	0.041	0.034	59	19
12	-0.040	0.030	-0.028	0.027	58	25
13	-0.085	0.030	0.011	0.024	36	8
14	-0.002	0.025	0.0026	0.022	11	360
15	0.010	0.031	0.012	0.032	65	104

Shear strain rates greater than 0.04 ppm/yr are shown in bold.

original angular measurements is 0.6 seconds of arc. Thus, combining three angular measurements to estimate the strain of a single triangle (the minimum number of measurements for estimating strain of an area) would be expected to yield an uncertainty of about 1 second of arc, or 0.04 ppm/yr over 126 years. Uncertainties for the strain rates in polygon regions (Table 1) are all at, or below, this level, demonstrating that regions of inconsistent strain have not been lumped together.

[13] The predominant feature in Figure 3 is the consistent NE-SW orientation of the principal axes. This observation, coupled with small values of the γ_2 strains (Table 1), strongly suggests that the first-order strain field is dominated by extension or contraction in the direction perpendicular to the axis of the Apennine chain. Statistically insignificant and inhomogeneous deformation is observed along the Tyrrhenian coast, where earthquakes barely exceed magnitude 4. The axis of the Apennines shows a continuous belt of active deformation with positive γ_1 and NE-SW-directed extensional principal strain axes. γ_1 strain rates range between 0.06 and 0.10 ppm/yr. Shear strains on the Adriatic side of the Apennines show predominantly negative γ_1 strain, though only the Gargano promontory shows a strain that is significantly greater than the noise. The large negative γ_1 strain and NE directed principal strain axis occurs in an area where large historical earthquakes and active faults have been described and mapped [Valensise and Pantosti, 2001]. In summary the main results show that active extensional deformation is concentrated along the axis of the Apennines in a belt 30–50 km wide, corresponding to the location of large earthquakes and elevated topography. The extension rate along the Apennines, under the assumptions that the observed shear strains reflect only NE-SW extension and that the belt of deformation is 30–50 km wide, ranges between 2.5 and 5 mm/yr (Table 2).

4. Comparison With Seismic Strain

[14] For each polygon that spans the Apennines (Table 2), we derived seismic strains following Kostrov [1974]:

$$\epsilon_{ij} = \frac{1}{2\mu V} \sum_1^n M_{ij} \quad (3)$$

Table 2. Extension Rate in the Polygons Along the Apennines

Poly.	Width (km)	Ext. Rate (mm/yr)	1σ	Mo Geod 10^{18} Nm	Mo Seismic 10^{18} Nm
6	50	2.5	1.4	27	2.9
7	30	3.5	1.0	25	1.9
8	30	2.9	1.5	12	8.2
9	40	3.1	1.1	34	11
10	50	5.0	1.0	51	24

Scalar geodetic moment is obtained by inverting equation 3.

where the ij^{th} component of the seismic strain tensor is derived from the summed moment tensors (M_{ij}) of earthquakes occurring in the volume (V), defined by the seismogenic layer (assumed to be 10 km thick) beneath the polygons; seismic strain rates are obtained by dividing by the interval of observation (126 years). The rigidity modulus (μ) is assumed here to be $2.8 \cdot 10^{10}$ N/m². The moment tensors of the earthquakes of the past century have all been determined instrumentally either from geodetic results and/or from standard seismological procedures. We allow a conservative 30% uncertainty in the estimate of M_{ij} . Under the assumptions above, we may convert our geodetic estimates of shear strain into estimates of the geodetic strain tensor: $\epsilon_{11} \sim \gamma_1$, $\epsilon_{22} \sim 0$, $\epsilon_{12} = \gamma_2/2$ and, assuming incompressibility, $\epsilon_{33} = -(\epsilon_{11} + \epsilon_{22})$. We may then use equation (3) in the inverse sense to convert geodetic measures of strain in polygons into equivalent seismic moments. Using this approach, we can make comparisons between the geodetic and seismic measures of strain. In this comparison, the Gargano Promontory is excluded because of the considerable uncertainties in the present-day tectonic regime. A potential source of error in this approach is that the geodetic strain tensor is uncertain by a dilatation (isotropic strain) which, in principle, could have any magnitude. In practice, we have set the scale in the 1875 network by assuming negligible linear strain in the direction parallel to the Apennine chain. Seismic strain observations show this to be a reasonable assumption, so we do not expect the error introduced by this approximation to be significant in comparison with the other sources of uncertainty.

[15] 4 shows the principal seismic strain rate axis for each polygon of Table 2 and a comparison between seismic and geodetic moments expressed as the difference (geodetic minus seismic) between the two scalar values. We note a general consistency between the two estimates (geodetic and seismic) of principal strain rate orientation. The combined uncertainties in the seismic and geodetic data are broad enough to permit the possibility that significant discrepancies in strain magnitude exist all along the Apennine chain. In particular, the discrepancy between geodetic and seismic strain in polygons 7 and 10 is at least as large as 2×10^{19} Nm, equivalent to a $M_w \sim 6.8$ earthquake.

5. Conclusions

[16] A 126-year geodetic measurement of shear strains shows that the deformation of peninsular Italy is largely confined to a region a few tens of kilometres wide that spans

the topographically highest and seismically most active part of the Apennine chain (Figure 3). The average strain rates across this region are at the level of 0.06 to 0.11 ppm/yr.

[17] Our results agree with the upper bound of 0.12 ppm/yr that *Hunstad and England* [1999] placed on the average strain rate of the Apennines. We can now be fairly confident that regional extensional rates across the Apennines are in the range of 2.5 to 5 mm/yr and that rates in the range of 10 mm/yr, as have been suggested by *Westaway* [1992], are inconsistent with the hundred-year geodetic record.

[18] The baseline lengths of the original geodetic network are too long (30–50 km) to allow us address rates of strain accumulation at the scale of individual faults or fault systems. Questions related to tectonics on the scale of 30 km or less will have to await data from denser GPS-to-GPS networks.

[19] **Acknowledgments.** We thank the IGM and ASI for access to the data. We thank Elisabetta D’Anastasio for her help during the project and Alessandro Amato for helpful discussion. We also thank Barbara Castello, Jeremy Hyde, Sergio Del Mese, Barry Parsons, Craig Allison and Luciano Giovanni and all the people that were with us in the field. Marco Anzidei provided some of the instruments and helpful logistics, and we acknowledge support from the Natural Environment Research Council through its Geophysical Equipment Pool, and COMET. We also thank Civil Protection and the pilot Carlo Geri for his skill in flight over mountain tops. This work is partially funded by the Civil Protection “GNDT” project “Probable earthquakes in Italy between the year 2000 and 2030: guidelines for determining priorities in seismic risk mitigation”.

References

- Anzidei, M., P. Baldi, G. Casula, A. Galvani, E. Mantovani, A. Pesci, F. Riguzzi, and E. Serpelloni, Insights into present-day crustal motion in the central Mediterranean area from GPS surveys, *Geophys. J. Int.*, *146*, 98–110, 2001.
- Cross, P. A., Practical integration of GPS and classical control networks, paper presented at XIX FIG Congress, Helsinki, 1995.
- D’Agostino, N., R. Giuliani, M. Mattone, and L. Bonci, Active crustal extension in the central Apennines (Italy) inferred from GPS measurements in the interval 1994 and 1999, *Geophys. Res. Lett.*, *28*(10), 2121–2124, 2001.
- Frank, F., Deduction of strains from survey data, *Bull. Seismol. Soc. Am.*, *56*, 35–42, 1966.
- Hunstad, I., and P. C. England, An upper bound on the rate of strain in central Apennines, Italy, from triangulation measurements between 1869 and 1993, *Earth Planet. Sci. Lett.*, *169*, 261–267, 1999.
- Kostrov, V. V., Seismic moment and energy of earthquakes, and seismic flow of rock, *Izv. Acad. Sci. USSR Phys. Solid Earth, Engl. Transl.*, *1*, 23–44, 1974.
- McKenzie, D., Active tectonics of the Mediterranean region, *Geophys. J. R. Astron. Soc.*, *30*, 109–185, 1972.
- Selvaggi, G., Spatial distribution of horizontal seismic strain in the Apennines from historical earthquakes, *Ann. Geofis.*, *41*, 241–251, 1998.
- Surace, L., La nuova rete geodetica fondamentale e il sistema IGM83, *Boll. Geod. Sci. Affini*, *LI*, 251–290, 1992.
- Valensise, and Pantosti, (Eds.), Database of potential sources for earthquakes larger than M5.5 in Italy, *Ann. Geofis.*, *44*, suppl. 1, 2001.
- Westaway, R., Seismic moment summation for historical earthquakes in Italy: Tectonic implications, *J. Geophys. Res.*, *97*, 15,437–15,464, 1992.
- Zumberge, J. F., M. B. Hefflin, D. C. Jefferson, M. M. Watkins, and F. H. Webb, Precise point positioning for the efficient and robust analysis of GPS data from large networks, *J. Geophys. Res.*, *102*, 5005–5017, 1997.
- N. D’Agostino, I. Hunstad, and G. Selvaggi, Istituto Nazionale di Geofisica e Vulcanologia, 00143 Rome, Italy.
- P. England, Department of Earth Sciences, Oxford University, Oxford, UK.
- P. Clarke, School of Civil Engineering and Geosciences, Newcastle, UK.
- M. Pierozzi, Istituto Geografico Militare, Florence, Italy.